

# Synthesis and Biological Evaluation of *N*<sup>1</sup>-(Anthracen-9-ylmethyl)triamines as Molecular Recognition Elements for the Polyamine Transporter

Chaojie Wang,<sup>†,‡</sup> Jean-Guy Delcros,<sup>§</sup> John Biggerstaff,<sup>†</sup> and Otto Phanstiel, IV<sup>\*,†</sup>

Groupe de Recherche en Thérapeutique Anticancéreuse, Faculté de Médecine, 2, Avenue du Professeur Léon Bernard, 35043 Rennes, France, and Department of Chemistry, P.O. Box 162366, University of Central Florida, Orlando, Florida 32816-2366

Received January 16, 2003

An efficient modular synthesis of *N*<sup>1</sup>-substituted triamines containing different tether lengths between nitrogen centers was developed. A series of *N*<sup>1</sup>-(9-anthracenylmethyl)triamines were evaluated for biological activity in L1210 (murine leukemia),  $\alpha$ -difluoromethylornithine (DFMO)-treated L1210, Chinese hamster ovary (CHO), and CHO-MG cell lines. All triamines **8** had increased potency in DFMO-treated L1210 cells. The 4,4- and 5,4-triamine systems had the highest affinity for the polyamine transporter (PAT) with L1210 *K*<sub>i</sub> values of 1.8 and 1.7  $\mu$ M, respectively. This trend was also reflected in the CHO studies. Surprisingly, the respective 4,4- and 5,4-triamine systems had 150-fold and 38-fold higher cytotoxicity in CHO cells containing active polyamine transporters. Initial microscopy studies revealed the rapid formation of vesicular structures within A375 melanoma cells treated with the *N*<sup>1</sup>-(9-anthracenylmethyl)homospermidine (4,4-triamine) conjugate. In summary, the 4,4- and 5,4-triamines were identified as selective vector motifs to ferry anthracene into cells via the PAT.

## Introduction

One of the major shortcomings of current cancer therapies is the nonselective delivery of the antineoplastic drug to both targeted tumor cells and healthy cells. Enhanced selectivity of such drugs could diminish their associated toxicity by reducing their uptake by healthy cells. Moreover, selective delivery would increase drug potency by lowering the effective dosage required to kill the affected cell type. Vector systems, which have enhanced affinity for cancer cells, would be an important advance in cancer chemotherapy. This report illustrates the development of conjugates between toxic agents and polyamines as one such vector system (see Figure 1).

The long-range goal of this research is to harness the polyamine transporter (PAT, a cell surface protein) for selective drug delivery.<sup>1,2</sup> The selection process would occur during the molecular recognition events involved in the import of exogenous polyamines by cancer cells.<sup>3–5</sup> In vivo, the polyamines exist as polycations (because the nitrogens are protonated at physiological pH) and are required for cell growth. Their alignment of point charges is recognized by the PAT and has been shown to facilitate their import.<sup>5</sup> Rapidly dividing cells require large amounts of polyamines in order to grow. These can be internally biosynthesized and also imported from exogenous sources. The high specific activity of polyamine transport in tumor cells is thought to be associated with the “inability of biosynthetic enzymes to provide sufficient levels of polyamines to sustain the rapid cell division.”<sup>6</sup> These bioproduction constraints are

partially offset by scavenging polyamines from exogenous sources.<sup>7</sup> In fact, many tumor types have been shown to contain elevated polyamine levels and an active PAT for importing exogenous polyamines. These range from neuroblastoma, melanoma, human lymphocytic leukemia, colonic, and lung tumor cell lines to murine L1210 cells.<sup>6</sup> In short, targeting of cancerous cell types would stem from their enhanced need for these biological growth factors.

To date, the transport of polyamines into mammalian cells is a measured<sup>1,2,5</sup> yet poorly understood phenomena. While significant work has also been accomplished in *E. coli*,<sup>3,4,8,9</sup> yeast,<sup>10</sup> and other systems,<sup>11</sup> the proteins involved in mammalian polyamine transport have not yet been isolated and characterized beyond a kinetic description. Clearly, the lack of structural detail associated with the mammalian transporter is a glaring void in the current knowledge base.

How can one design a polyamine vector to utilize a transporter of unknown structure? Several authors have developed structure–activity relationships to indirectly address this issue.<sup>1,2,5,12</sup> Thus far, small structural changes have resulted in dramatic differences in the transport behavior of polyamine analogues. For example, a single methylene (CH<sub>2</sub>) unit change in the tether separating the nitrogen centers has been shown to significantly alter analogue uptake.<sup>5</sup> This report focuses on the unsymmetrical linear polyamines, which are *N*-substituted at only one end of the polyamine chain. While the terminally bis-alkylated polyamines have yielded diverse biological activity ranging from anticancer to antidiarrheal agents,<sup>5,11</sup> their monosubstituted analogues have limited publications describing their use in vector design.<sup>1,2,5,13–21</sup> This, in part, may stem from their less direct syntheses, which involve several steps.<sup>5,19</sup> In fact, only a few efficient syntheses

\* To whom correspondence should be addressed. E-mail: ophansti@mail.ucf.edu. Phone: (407) 823-5410. Fax: (407) 823-2252.

<sup>†</sup> University of Central Florida.

<sup>‡</sup> C.W. is a visiting scholar from the Department of Chemistry, Henan University, Kaifeng, 475001, P. R. China.

<sup>§</sup> Groupe de Recherche en Thérapeutique Anticancéreuse, Faculté de Médecine.

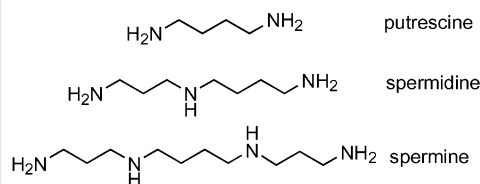
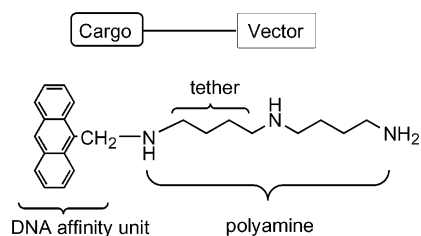


**Figure 1.** Sample conjugate system and the native polyamines.

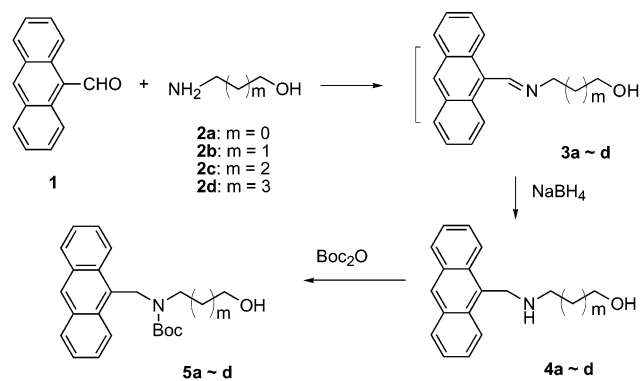
of unsymmetrically substituted polyamines were published prior to 1993.<sup>22</sup>

There are several caveats to using polyamines to selectively deliver toxic “cargoes”. First, rapidly dividing normal cell types (e.g., bone marrow, intestinal epithelium, and hair follicles) may also be affected by this strategy. Whether polyamine conjugates can discriminate between cancer cell types and these other prolific cell lines remains to be seen. Nevertheless, other authors have observed that transformed cells are more sensitive than normal cells to  $\alpha$ -difluoromethylornithine (DFMO) pretreatment. DFMO is a known ornithine decarboxylase (ODC) inhibitor. ODC is responsible for putrescine biosynthesis, and its inhibition has been shown to increase the uptake of extracellular polyamines.<sup>23</sup> Most pertinent to this study is the observation that when DFMO is dosed in vivo, it increased the uptake of radiolabeled putrescine specifically into tumor cells and not into other normal tissue, even rapidly growing tissue.<sup>23</sup> This suggests that DFMO treatment may also increase the potency of the present polyamine conjugates. Second, the “cargoes” to be delivered in this study (e.g., anthracene derivatives) are relatively inert. It is possible that other anticancer agents or “cargoes”, which have more reactive chemical entities, may interact with PAT or other cell surface receptors and diminish the anticipated selectivity. In this report, our goal was not to develop new anticancer agents per se but to use a stable model architecture (anthracene) in order to understand which polyamine sequence was best able to access the PAT.

The conjugates in this report are dualistic in design and comprise an anthracene nucleus covalently bound to a polyamine framework. In this manner, cells will be challenged to import the same lethal cargo (anthracene) using a modified polyamine motif (for cellular entry via the PAT).<sup>1,2</sup> The anthracene component was selected because of significant preliminary data, which revealed its increased potency over an acridine analogue in murine leukemia (L1210) cells.<sup>1,2</sup> Moreover, the anthracene provides a convenient UV “probe” for compound identification and elicits a toxic response from cells upon entry (presumably through DNA coordination).<sup>24</sup> Early studies had revealed that branched polyamines have moderate affinity for the PAT and can provide access to cells.<sup>1,2</sup> However, recent data suggested that the linear polyamines were superior vectors over their branched counterparts.<sup>12</sup> In this manner, a series of polyamine–anthracene conjugates were synthesized and screened for uptake via the PAT.

By judicious choice of amine substrates (e.g., a synthetic library) and proper biological experiments (e.g.,  $IC_{50}$  and  $K_i$  measurements) for selected cell types (murine leukemia L1210, CHO, and CHO-MG cells), one

### Scheme 1



can now comment on transport affinity and potency as a function of polyamine–drug conjugate structure.

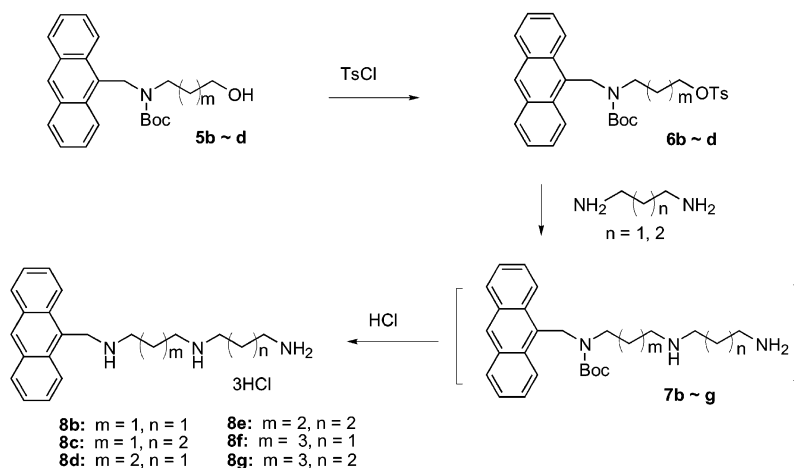
### Synthesis

As shown in Scheme 1, the reductive amination of **1** to **4** was achieved in two steps via in situ generation of the imine **3**. A homologous series of imines (**3a–d**) were prepared from **1** and different amino alcohols. Each imine was then reduced to its respective amine **4** with  $NaBH_4$  in good yield without purification. Solvent removal by rotary evaporation at 40–50 °C facilitated imine formation and provided satisfactory yields of the 2° amines, **4a–d**, (68–81%) after the two-step process. The 2° amines **4a–d** were *N*-protected to form **5** using excess di-*tert*-butyl dicarbonate,  $Boc_2O$ . Interestingly, compound **5b**, which contained three methylene units, was unstable, even when it was stored at low temperature (0–5 °C) under nitrogen. This finding is in direct contrast to **5a**, **5c**, and **5d**, which were stable at room temperature.

In the seemingly routine tosylation step, shown in Scheme 2, we were unable to obtain the desired compound **6a** from the *N*-Boc protected **5a**. Tosylate **6b** was isolated in lower yield (51%) but was unstable to prolonged storage. In contrast, tosylates **6c** and **6d** were prepared in higher yields (88%) and were relatively stable. However, their respective colors and  $^1H$  NMR spectra slowly changed during prolonged storage in the refrigerator. Therefore, the tosylates **6** were best generated and used as soon as possible.

Interesting  $^1H$  NMR behavior was observed for **5a–c**. The *N*-Boc protection of **4** led to the expected downfield shift of the “benzylic  $CH_2$ ” from  $\delta \sim 4.7$  in **4** to  $\delta \sim 5.5$  in **5** because of the inductive effects of the Boc group. However, the non-benzylic  $N^1-CH_2$  in **5a–c** and the other  $CH_2$  units were all shifted upfield (especially the  $CH_2-O$  group, e.g.,  $\delta$  3.80 in **4b** to  $\delta$  3.25 in **5b**). A similar chemical shift change had been observed with a series of *N*-tosyl-*N*-anthracenylmethylpolyamine de-

## Scheme 2



rivatives.<sup>25</sup> These derivatives revealed a novel orientation wherein the polyamine “tail” was oriented over the shielding cone of the anthracene ring presumably because of the steric effects of the *N*-tosyl group. The *N*-Boc derivatives **5a–c** also seem to adopt this unusual orientation, which results in the unexpected upfield chemical shifts. However, this structural feature disappeared upon O-tosylation of **5** to form **6**.

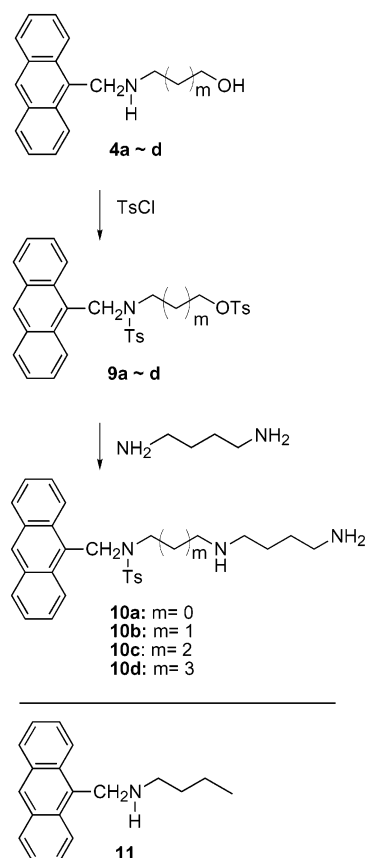
The tosylated compounds (**6b–d**) were reacted with excess putrescine or 1,3-diaminopropane to form the six *N*<sup>1</sup>-Boc protected triamines **7b–g**. These triamines were isolated but were again unstable to prolonged storage at low temperature. Therefore, they were consumed in the next step immediately after purification. The *N*-Boc groups of **7** were removed by 4 N HCl, and the six target compounds **8b–g** were formed in good yield. Impurities in **8** were removed simply by washing the solids with absolute ethanol.

As shown in Scheme 3, derivatives **4a–d** were previously converted to their respective *N,O*-bistosylates, **9a–d**.<sup>25</sup> Displacement of the terminal tosylate by butanediamine provided the series **10a–d** in good yield.<sup>25</sup> Derivatives **10a–d** represent triamine systems containing two large aromatic “cargoes” and have one of the terminal amines sequestered as a sulfonamide. In addition, the *N*-(anthracen-9-ylmethyl)-*N*-butylamine HCl salt (**11**) shown in Scheme 3 was synthesized in 58% yield by reductive amination of 9-anthraldehyde and butylamine followed by treatment with 4 N aqueous HCl. Compound **11** was an important control because it represented a charged anthracene moiety without an attached polyamine vector. How these large structural perturbations influence the cytotoxicity of the bioconjugate were evaluated via IC<sub>50</sub> determinations.

## Biological Evaluation

Three cell lines were chosen for bioassay. L1210 (mouse leukemia) cells were selected to enable comparisons with the IC<sub>50</sub>, and *K<sub>i</sub>* values were determined previously for a variety of polyamine substrates.<sup>5,26</sup> Chinese hamster ovary (CHO) cells were chosen along with a mutant cell line (CHO-MG) in order to comment on how the synthetic conjugates gain access to cells.<sup>12</sup> The CHO-MG cell line is polyamine-transport-deficient and was isolated after chronic selection for growth resistance to methylglyoxalbis(guanylhydrazine).<sup>27</sup> For

## Scheme 3



the purposes of this study, the CHO-MG cell line represents cells with very low PAT activity and provides a model for alternative modes of entry or action. These alternative modes of entry, which are non-PAT-based, include passive diffusion or utilization of another transporter. The alternative modes of action may include interactions on the outer surface of the plasma membrane or other membrane–receptor interactions. In contrast, the parent CHO cell line represents a cell type with high PAT activity.<sup>27,28</sup> Comparison of efficacy in these two lines provided an important screen to detect selective conjugate delivery via the PAT. For example, a conjugate with high utilization of the polyamine transporter would be very toxic to CHO cells but less so to CHO-MG cells.<sup>12,27</sup> Therefore, IC<sub>50</sub> determination

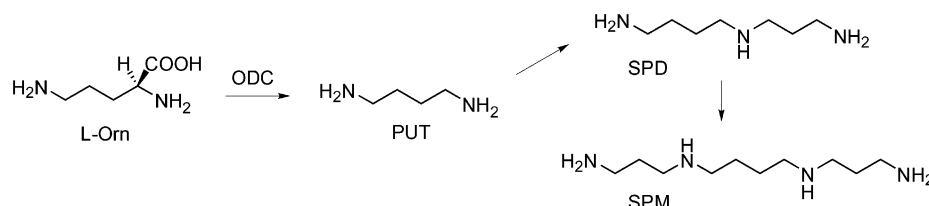


**Figure 2.** Polyamine biosynthetic pathway.

**Table 1.** Biological Evaluation of Triamines **8b–g**, *N*-Tosyl Derivatives **10a–d**, and **11** in L1210 Cells<sup>a</sup>

compd (tether)	L1210 IC <sub>50</sub> (μM)	L1210 + DFMO IC <sub>50</sub> (μM)	L1210/(L1210 + DFMO) IC <sub>50</sub> ratio	L1210 K <sub>i</sub> (μM)
<b>8b</b> (3,3)	1.8 ± 0.4	1.4 ± 0.3	1.3	33.4 ± 2.6
<b>8c</b> (3,4)	0.7 ± 0.3	0.3 ± 0.1	2.3	2.5 ± 0.3
<b>8d</b> (4,3)	0.4 ± 0.1	0.2 ± 0.02	2	6.2 ± 0.6
<b>8e</b> (4,4)	0.3 ± 0.04	0.15 ± 0.1	2	1.8 ± 0.1
<b>8f</b> (5,3)	1.3 ± 0.1	0.7 ± 0.1	1.9	5.0 ± 0.6
<b>8g</b> (5,4)	0.4 ± 0.1	0.3 ± 0.1	1.3	1.7 ± 0.2
<b>10a</b> (2,4)	3.3 ± 0.2	3.9 ± 0.9	0.9	ND
<b>10b</b> (3,4)	6.3 ± 0.5	7.7 ± 1.1	0.8	ND
<b>10c</b> (4,4)	7.4 ± 1.0	8.1 ± 1.6	0.9	ND
<b>10d</b> (5,4)	6.2 ± 0.3	6.9 ± 0.8	0.9	ND
<b>11</b> ( <i>N</i> -butyl)	14.6 ± 0.1	21.9 ± 3.6	0.7	62.3 ± 4.2

<sup>a</sup> Individual L1210 IC<sub>50</sub> values are listed in μM, and the IC<sub>50</sub> ratio is dimensionless. ND = not determined.

in these two CHO lines provided a relative ranking of delivery via the PAT. In short, highly selective, vectored conjugates should give high CHO-MG/CHO IC<sub>50</sub> ratios.

As mentioned previously, DFMO is a known ODC inhibitor.<sup>29</sup> ODC is the enzyme responsible for the biosynthesis of putrescine from L-ornithine (see Figure 2). Putrescine (PUT) is then converted to the longer polyamines, spermidine (SPD) and spermine (SPM), via successive aminopropylation steps (Figure 2). Inhibition of ODC blocks intracellular putrescine biosynthesis and leads to a significant increase in polyamine uptake, which allows the cell to acquire polyamines from exogenous sources. Therefore, cells that are treated with DFMO should be more susceptible to the polyamine-vectored conjugates and should provide lower IC<sub>50</sub> values.<sup>11,12</sup> IC<sub>50</sub> values for L1210 cells with and without DFMO treatment were determined. Conjugates, which selectively target the PAT, should be more potent with DFMO-treated cells and should provide L1210/(L1210 + DFMO) IC<sub>50</sub> ratios greater than 1.

All the derivatives listed in Table 1 (e.g., **8b–g**, **10a–d**, and **11**) were cytotoxic to L1210 cells and had IC<sub>50</sub> values less than 15 μM. The DFMO-treated L1210 cells were more susceptible to conjugates **8b–g** than the sulfonamides **10** or control **11**. This finding suggests that conjugates such as **8** use the PAT to enter cells. DFMO treatment typically resulted in higher potency for **8** and other previous polyamine conjugates.<sup>12</sup> It should be noted that in the present study, the DFMO was coadministered with the polyamine conjugate and therefore DFMO's potency enhancement may not have been maximal. Nevertheless, our findings are consistent with those of other authors.<sup>12</sup>

The K<sub>i</sub> values in Table 1 reflect the affinity of the polyamine derivative for the polyamine transporter on the cell surface. Conjugates with an appended 4,4-triamine (**8e**) or 5,4-triamine (**8g**) sequence had the lowest K<sub>i</sub> values (1.8 and 1.7 μM, respectively) and, therefore, the highest affinity for the L1210 polyamine transporter. A comparison of **8e** and **8g** with the *N*-(anthracen-9-ylmethyl)butylamine control **11** (K<sub>i</sub> =

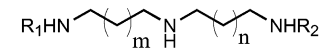
**Table 2.** Biological Evaluation of Triamines **8b–g**, *N*-Tosyl Derivatives **10a–d**, and **11** in the CHO-MG and CHO Cell Lines

compd (tether)	CHO-MG IC <sub>50</sub> (μM)	CHO IC <sub>50</sub> (μM)	CHO-MG/CHO IC <sub>50</sub> ratio
<b>8b</b> (3,3)	3.4 ± 0.5	1.9 ± 0.4	1.8
<b>8c</b> (3,4)	8.8 ± 1.2	2.5 ± 0.7	3.5
<b>8d</b> (4,3)	9.5 ± 1.1	0.4 ± 0.1	24
<b>8e</b> (4,4)	66.7 ± 4.1	0.45 ± 0.1	148
<b>8f</b> (5,3)	10.1 ± 1.2	4.1 ± 0.5	2.5
<b>8g</b> (5,4)	57.3 ± 2.9	1.5 ± 0.1	38
<b>10a</b> (2,4)	7.1 ± 0.4	5.1 ± 0.6	1.4
<b>10b</b> (3,4)	11.1 ± 1.3	10.2 ± 0.9	1.1
<b>10c</b> (4,4)	10.6 ± 1.9	10.4 ± 1.6	1.0
<b>10d</b> (5,4)	7.8 ± 1.9	7.1 ± 0.8	1.1
<b>11</b> ( <i>N</i> -butyl)	11.2 ± 2.3	10.5 ± 2.0	1.1

62.3 μM) revealed the significantly higher PAT affinity (lower K<sub>i</sub> values) of conjugates containing a preferred polyamine sequence. Although control **11** was able to kill cells, it did so with lower potency than the vectored systems **8e** and **8g**. This finding is significant because it suggests that the 4,4- or 5,4-triamine motif selectively vectored the anthracene cargo into cells via the PAT. This selectivity became very apparent in the latter CHO studies.

As shown in Table 2, biological evaluation of triamines **8b–g**, **10a–d**, and **11** in the two CHO cell lines revealed striking preferences by certain polyamine architectures for the PAT. Perhaps most exciting was the fact that the 4,4-triamine **8e** displayed a nearly 150-fold preference for the CHO over the CHO-MG cell line. In contrast, the 3,3-triamine analogue **8b** preferred this line by only 1.8-fold. These findings demonstrate that CHO and CHO-MG IC<sub>50</sub> comparisons are an excellent way to rank polyamine vectors and their transport.<sup>12</sup> The effectiveness of the triamines **8e** and **8g** correlated nicely with the L1210 IC<sub>50</sub> and K<sub>i</sub> results, wherein each had enhanced potency with DFMO-treated cells and high affinity for the polyamine transporter. Indeed, the triamine systems (**8e** and **8g**) seem to be well-behaved systems, which give consistent data in all three cell lines.



**Table 3.** L1210 IC<sub>50</sub> and K<sub>i</sub> Data<sup>5</sup>


entry no.	R <sub>1</sub>	R <sub>2</sub>	m	n	IC <sub>50</sub> (μM, 96 h)	K <sub>i</sub> (μM)
1	propyl (Pr)	Pr	1	1	60	125
2	Pr	H	1	1	100	33
3	Pr	Pr	1	2	33	26
4	Pr	H	1	2	28	3
5	H	Pr	1	2	55	8.5
6	Pr	Pr	2	2	6	67
7	Pr	H	2	2	0.6	5

The *N*-tosyl derivatives **10a–d** and the control **11** demonstrated similar potency in both the CHO-MG and CHO cell lines (with IC<sub>50</sub> values ranging from 5.1 to 11.2 μM). These findings suggested that these particular analogues are entering the cell via a non-PAT-mediated pathway to elicit their toxic response. Nevertheless, the vectored polyamine conjugates (**8e** and **8g**) were significantly less potent in the CHO-MG cell line (IC<sub>50</sub> = 66.7 and 57.3 μM, respectively) versus the control **11** (IC<sub>50</sub> = 11.2 μM). Therefore, certain polyamine architectures (like those found in **8e** and **8g**) can alter the uptake characteristics of the appended anthracene. Indeed, the proper polyamine sequence imparted high selectivity for the PAT.

Another way of illustrating this selectivity enhancement is to consider the differences in hydrophobicity between the control **11** and the triamine derivatives **8b–g**. Hydrophobic compounds (like **11**) should be expected to permeate across the cell membrane without the use of a specific transport system. In contrast, the appended polyamine motif in **8** should significantly reduce the hydrophobicity of these conjugates. If one assumes that each triamine motif (existing as a polyammonium tail) imparts similar water solubility to the appended anthracene, then one would anticipate that **8b–g** would all give the same biological data in Table 2. This is clearly not the case (e.g., **8b** vs **8e**). Therefore, the data cannot be explained by a simple change in hydrophobicity. Instead, the dramatic differences observed in the CHO cell lines are more consistent with the attachment of a selective molecular recognition element for a particular cell surface receptor (i.e., the PAT).

Other authors have shown differences in transport affinity (K<sub>i</sub>) and cytotoxicity (IC<sub>50</sub>) behavior for the *N,N*-dialkylpolyamine and *N*-monoalkylpolyamine architectures.<sup>5</sup> In an elegant study by Bergeron et al., the monopropylpolyamine derivatives gave lower K<sub>i</sub> values than their dialkylated counterparts (Table 3).<sup>5</sup> However, in some cases, this property did not always correlate with higher potency (e.g., IC<sub>50</sub> values for entries 1 and 2 in Table 3). Subtleties in tether length were also apparent. For example, as shown in Table 3, the 3,4 triamine system (entry 4) had a lower K<sub>i</sub> than its 4,3 counterpart (entry 5). A similar trend was observed in Table 1 with **8c** and **8d**. Therefore, the polyamine transporter is capable of distinguishing between isomeric systems that have the same overall length but a different separation of point charges.<sup>5,30–34</sup> Indeed, the current study has identified some of the optimal motifs in order to initiate transport via this pathway.

In terms of vector design, the monoalkylated polyamine motif is more attractive because cells seem capable of

importing large “cargoes” as long as they are tethered at only one end.<sup>6,12</sup> The 4,4-triamine **8e** represents a potential “home run” for these vectored systems in terms of its potential 150-fold selectivity and observed low IC<sub>50</sub> values in the CHO and L1210 cell lines (Tables 1 and 2). Comparisons between the CHO and CHO-MG cell lines (i.e., respective IC<sub>50</sub> values) provided a sensitive screen for identifying architectures, which are more specific for the PAT. Recall that in the proposed model, the CHO cells represent cell types with active polyamine transporters and the CHO-MG cell line represent cells with low PAT activity. The observed 150-fold selectivity in distinguishing between these two cell lines represents a major advance in polyamine vector design. In short, certain polyamine vectors can selectively deliver “large” toxic agents to cells with highly active polyamine transporters.

Another outcome of this study was use of **8b–g** as new polyamine probes that have differential affinity for the PAT and are fluorescent. In this regard, the conjugates (**8**) could be tracked by deconvolution microscopy.

### Deconvolution Microscopy

Recently other authors have suggested two mechanisms for polyamine transport into mammalian cells (e.g., via receptor-mediated endocytosis or via a protein channel).<sup>6,35</sup> Of the two, the receptor-mediated endocytosis pathway had the greatest experimental support.<sup>6,35</sup> For example, Cullis reasoned that a rigid protein channel with a fixed diameter would be sensitive to steric effects at either end of the polyamine chain. An envagination process, however, would be more tolerant of bulky “cargoes” appended to the polyamine vector. Indeed, Cullis concluded that the polyamine transporter has a “surprising broad structural tolerance”.<sup>6</sup>

One of the limitations of the above biochemical assays is that they are indirect measurements and do not provide cellular localization information. Where do the conjugates go once they enter the cell? Conjugate localization information could help explain both the mechanism of action of these systems and their transport behavior. Deconvolution microscopy offered a unique ability to address this question. By the synthesis of conjugates with dramatically different transport properties (e.g., **8b** vs **8e**), this project generated important probes for studying transport phenomena. The anthracene moiety offers a convenient UV “handle” to monitor the location of the drug conjugate within the cell. The UV spectra of these anthracene conjugates suggest a consistent λ<sub>max</sub> near 364 nm and an emission maxima near 417 nm. As shown in Figure 3, when A375 melanoma cells are incubated for 3 min with 10 μM **8e**, deconvolution microscopy revealed the rapid formation of fluorescent vesicles (containing **8e**) within the cell. Control experiments with water or DMSO were “dark” and gave no fluorescence with this filter set. These results are exciting because they suggest that the homologous series **8** could be used as fluorescent probes to study polyamine uptake.

Our findings are consistent with those reported by the Cullis and Poulin groups, which also observed the formation of vesicles and suggested receptor-mediated endocytosis as a mode of transport for both a *N*-

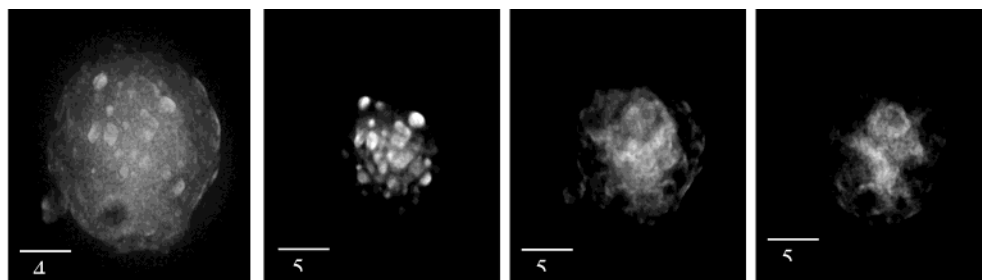


**Figure 3.** Deconvolution microscopy images of an A375 cell treated with **8e** (10  $\mu$ M). This technique provides an image of the entire cell by using software to overlay a series of planar images (or slices) to give a stacked translucent view of the entire cell (leftmost image above). The lightest regions contain the highest concentration of the fluorescent agent **8e**. The three representative slices (second from left, second from right, and rightmost images) were chosen from a total of 32 images. A scale bar is shown in micrometers.

methylanthranilic acid (MANT)–polyamine conjugate<sup>6</sup> and a spermidine–C2-BODIPY conjugate.<sup>35</sup> Therefore, the sequestration of **8e** into vesicles (along with similar findings by other investigators) supports an endocytotic process.<sup>6,35</sup> Whether other importation mechanisms are in play remains to be seen.

Future studies will relate PAT affinity and transport properties to a particular cellular compartmentalization/uptake process. An advantage of the present systems such as **8** is that the UV probe is also the toxic entity and not a UV prosthetic like MANT. Moreover, the *N*<sup>1</sup>-spermidine–MANT conjugate used by Cullis had a *K*<sub>i</sub> value of 23.4  $\mu$ M, which is over a log unit higher than the chlorambucil–polyamine conjugates they were modeling.<sup>6,20</sup> In the present case, the conjugate **8** itself is both the UV probe and the active drug. We are now poised to compare several members of the series in a time-lapse microscopy study, which will be the focus of a future report.

## Conclusions

An efficient modular synthesis of *N*<sup>1</sup>-substituted triamines containing different tether lengths between nitrogen centers was developed. This new methodology should contribute to the limited synthetic approaches used to access linear polyamines.<sup>36</sup> Triamine conjugates such as **8** had increased potency in DFMO-treated L1210 cells, whereas the related *N*<sup>1</sup>-tosyl derivatives **10** and control **11** did not. All polyamine vectors do not impart the same selectivity. Indeed, only a few of the screened triamines demonstrated the desired vectoring behavior. The 4,4- and 5,4-triamine systems had the highest affinity for the PAT with L1210 *K*<sub>i</sub> values of 1.8 and 1.7  $\mu$ M, respectively. A survey of different polyamine vectors revealed that the respective 4,4- and 5,4-triamine systems had 150-fold and 38-fold higher cytotoxicity in CHO cells containing active polyamine transporters. Initial microscopy studies revealed the rapid formation of vesicular structures within A375 melanoma cells treated with the *N*<sup>1</sup>-(9-anthracenylmethyl)homospermidine conjugate **8e**. In summary, the 4,4- and 5,4-triamines were identified as selective vector motifs for the PAT. Future work will also probe the influence of these conjugates on intracellular polyamine pools and enzymes.

## Experimental Section

**Materials.** Silica gel (32–63  $\mu$ m) and chemical reagents were purchased from commercial sources and used without further purification. All solvents were distilled prior to use.

<sup>1</sup>H NMR and <sup>13</sup>C NMR spectra were recorded at 300 and 75 MHz, respectively. TLC solvent systems are based on volume percent, and NH<sub>4</sub>OH refers to concentrated aqueous NH<sub>4</sub>OH. Elemental analyses were performed by Atlantic Microlabs (Norcross, GA). High-resolution mass spectrometry was performed by Dr. David Powell at the University of Florida Mass Spectrometry facility. The syntheses of *N*-tosyl derivatives **9** and **10** have been previously described.<sup>25</sup>

**Biological Studies.** Murine leukemia cells (L1210), CHO, and CHO-MG cells were grown in RPMI medium (Eurobio, Les Ulis, France) supplemented with 10% fetal calf serum, 2 mM glutamine (2 mM), penicillin (100U/mL), and streptomycin (50  $\mu$ g/mL) (BioMerieux, MArcl'Étoile, France). L-Proline (2  $\mu$ g/mL) was added to the culture medium for CHO-MG cells. Cells were grown at 37 °C under a humidified 5% CO<sub>2</sub> atmosphere. Aminoguanidine (2 mM) was added to the culture medium to prevent oxidation of the drugs by the enzyme (bovine serum amine oxidase) present in calf serum. Trypan blue staining was used to determine cell viability before the initiation of a cytotoxicity experiment. Typically, samples contained less than 5% trypan blue positive cells (dead). For example, L1210 cells in early to mid log phase were used.

**IC<sub>50</sub> Determinations.** Cell growth was assayed in sterile 96-well microtiter plates (Becton-Dickinson, Oxnard, CA). L1210 cells were seeded at 5  $\times$  10<sup>4</sup> cells/mL of medium (100  $\mu$ L/well). Single CHO and CHO-MG cells harvested by trypsinization were plated at 2  $\times$  10<sup>3</sup> cells/mL. Drug solutions (5  $\mu$ L per well) of appropriate concentration were added at the time of seeding for L1210 cells and after an overnight incubation for CHO and CHO-MG cells. In some experiments, DFMO (5 mM) was added in the culture medium at the time of drug addition. After exposure to the drug for 48 h, cell growth was determined by measuring formazan formation from 3-(4,5-dimethylthiazol-2-yl)-2,5-diphenyltetrazolium using a Titertek Multiskan MCC/340 microplate reader (Labsystems, Cergy-Pontoise, France) for absorbance (540 nm) measurements.<sup>37</sup>

**K<sub>i</sub> Procedure.** The ability of the conjugates to interact with the polyamine transport system was determined by measuring competition by the conjugates against radiolabeled spermidine uptake in L1210 cells. Initially, the *K<sub>m</sub>* value of spermidine transport was determined in a reaction volume of 600  $\mu$ L of Hanks' balanced salt solution (HBSS) containing 3  $\times$  10<sup>6</sup> cells/mL in the presence of 0.5, 1, 2, 4, 6, and 8  $\mu$ M [<sup>14</sup>C]-spermidine. The cell suspensions were incubated at 37 °C for 10 min. The reaction was stopped by adding 3 mL of ice-cold phosphate-buffered saline (PBS). The tubes were centrifuged, and the supernatant was removed. The cell pellets were then washed twice with ice-cold PBS, and the supernatant was removed. The pellet was broken by sonication in 500  $\mu$ L of 0.1% Triton in distilled water. Two hundred microliters of the cell lysate was transferred in a 5 mL scintillation vial containing 3 mL of Pico-Fluor 15. The respective radioactivity of each sample was measured using a scintillation counter. The *K<sub>m</sub>* value of spermidine transport was determined by Lineweaver–Burke analysis as described.<sup>38</sup>

The ability of conjugates to compete for [<sup>14</sup>C]-spermidine uptake was determined in L1210 cells by a 10 min uptake



assay in the presence of increasing concentrations of competitor, using 1  $\mu$ M [<sup>14</sup>C]-spermidine as substrate.  $K_i$  values for inhibition of spermidine uptake were determined using the Cheng-Prusoff equation<sup>39</sup> from the IC<sub>50</sub> value derived by iterative curve fitting of the sigmoidal equation describing the velocity of spermidine uptake in the presence of the respective competitor.<sup>40,41</sup> Cell lines (murine leukemic L1210 cells) were grown and maintained according to established procedures.<sup>7,42</sup> Cells were washed twice in HBSS prior to the transport assay.

**Deconvolution Microscopy.** The microscope system included an Applied Precision (Issaquah, WA) Deltavision system equipped with a Nikon Eclipse TE200 inverted microscope. Image deconvolution was performed using Applied Precision SoftWorX software. Detached melanoma A375 cells were prepared by 3 min incubation with trypsin. The cells were then washed, centrifuged and resuspended in phosphate buffered saline. The cells were then washed repetitively with fresh media, and the cells were fixed onto a microscope slide and imaged by the deconvolution microscope. This technique provides an image of the entire cell by using software to overlay a series of planar images (or slices) to give a stacked translucent view of the entire cell. The lightest regions contain the highest concentration of the fluorescent agent **8c**.

**General Procedure for the Synthesis of N-(Anthracen-9-ylmethyl)amino Alcohols, 4.** To a stirred solution of amino alcohol **2** (12 mmol) in 25% MeOH/CH<sub>2</sub>Cl<sub>2</sub> (10 mL) was added a solution of 9-anthraldehyde **1** (10 mmol) in 25% MeOH/CH<sub>2</sub>Cl<sub>2</sub> (10 mL) under N<sub>2</sub>. The mixture was stirred at room temperature overnight until the imine formation was complete (monitored by TLC). The solvent was evaporated under vacuum to give the crude imine **3** as a bright-green solid, which was used for reduction without further purification.

NaBH<sub>4</sub> (30 mmol) was added in small portions to a solution of imine **1:1** CH<sub>3</sub>OH/CH<sub>2</sub>Cl<sub>2</sub> (20 mL) at 0 °C. The mixture was stirred at room temperature overnight and then concentrated under vacuum. The residue was dissolved in CH<sub>2</sub>Cl<sub>2</sub> (50 mL) and washed three times with aqueous Na<sub>2</sub>CO<sub>3</sub> (pH 10, 50 mL). The organic layer was separated, dried over anhydrous Na<sub>2</sub>SO<sub>4</sub>, filtered, and concentrated under vacuum. The residue was purified by flash chromatography on silica gel.

**2-[(Anthracen-9-ylmethyl)amino]ethanol, 4a:** bright-yellow solid; mp 116–118 °C; yield 77%;  $R_f$  = 0.48, methanol/chloroform, 1:9; <sup>1</sup>H NMR (300 MHz, CDCl<sub>3</sub>)  $\delta$  8.40 (s, 1H), 8.28 (d, 2H), 8.00 (d, 2H), 7.48 (m, 4H), 4.68 (s, 2H), 3.64 (t, 2H), 3.00 (t, 2H), 2.1 (br s, 2H); <sup>13</sup>C NMR  $\delta$  131.75, 131.44, 130.45, 129.47, 127.63, 126.48, 125.23, 124.18, 61.12, 51.65, 45.41. Anal. (C<sub>17</sub>H<sub>17</sub>NO) C, H, N. HRMS (FAB)  $m/z$  calcd for C<sub>17</sub>H<sub>18</sub>NO (M + H)<sup>+</sup>: 252.1388. Found: 252.1381.

**3-[(Anthracen-9-ylmethyl)amino]propan-1-ol, 4b:** bright-yellow solid; mp 82–83 °C; yield 80%;  $R_f$  = 0.51, methanol/chloroform, 1:9; <sup>1</sup>H NMR (300 MHz, CDCl<sub>3</sub>)  $\delta$  8.40 (s, 1H), 8.28 (d, 2H), 8.00 (d, 2H), 7.46 (m, 4H), 4.70 (s, 2H), 3.80 (t, 2H), 3.10 (t, 2H), 2.90 (br s, 2H), 1.78 (m, 2H); <sup>13</sup>C NMR  $\delta$  131.72, 130.98, 130.48, 129.48, 127.72, 126.56, 125.25, 124.06, 64.65, 50.83, 46.02, 31.14. Anal. (C<sub>18</sub>H<sub>19</sub>NO) C, H, N. HRMS (FAB)  $m/z$  calcd for C<sub>18</sub>H<sub>20</sub>NO (M + H)<sup>+</sup>: 266.1545. Found: 266.1526.

**4-[(Anthracen-9-ylmethyl)amino]butan-1-ol, 4c:** bright-yellow solid; mp 87–88 °C; yield 81%;  $R_f$  = 0.51, methanol/chloroform, 1:9; <sup>1</sup>H NMR (300 MHz, CDCl<sub>3</sub>)  $\delta$  8.40 (s, 1H), 8.26 (d, 2H), 8.00 (d, 2H), 7.49 (m, 4H), 4.68 (s, 2H), 3.50 (t, 2H), 2.90 (t, 2H), 1.65 (br s, 4H); <sup>13</sup>C NMR  $\delta$  131.74, 130.73, 130.48, 129.51, 127.82, 126.64, 125.30, 123.96, 62.89, 50.58, 45.72, 32.72, 29.13. Anal. (C<sub>19</sub>H<sub>21</sub>NO) C, H, N. HRMS (FAB)  $m/z$  calcd for C<sub>19</sub>H<sub>22</sub>NO (M + H)<sup>+</sup>: 280.1701. Found: 280.1679.

**5-[(Anthracen-9-ylmethyl)amino]pentan-1-ol, 4d:** bright-yellow solid; mp 76–77 °C; yield 68%;  $R_f$  = 0.26, methanol/chloroform (5:95); <sup>1</sup>H NMR (CDCl<sub>3</sub>)  $\delta$  8.38 (s, 1H), 8.27 (d, 2H), 7.98 (d, 2H), 7.45 (m, 4H), 4.65 (s, 2H), 3.50 (t, 2H), 2.82 (t, 2H), 1.78 (br s, 2H), 1.50 (m, 4H), 1.40 (m, 2H); <sup>13</sup>C NMR (CDCl<sub>3</sub>)  $\delta$  131.89, 131.77, 130.48, 129.44, 127.46, 126.40, 125.19, 124.29, 62.68, 50.60, 45.96, 32.68, 29.91, 23.67. Anal. (C<sub>20</sub>H<sub>23</sub>NO) C, H, N. HRMS (FAB)  $m/z$  calcd for C<sub>20</sub>H<sub>24</sub>NO (M + H)<sup>+</sup>: 294.1858. Found: 294.1835.

**General Procedure for the Synthesis of N-Boc-N-(Anthracen-9-ylmethyl)amino Alcohols, 5.** The solution of N-(anthracen-9-ylmethyl)amino alcohol **4** (5 mmol) in 20 mL of pyridine/methanol (1:5 v/v) was stirred at 0 °C for 10 min. A solution of di-*tert*-butyl dicarbonate (7.5 mmol) in methanol (5 mL) was added dropwise over 10 min. The temperature was allowed to rise to room temperature and the reaction mixture was stirred overnight. The mixture was evaporated to dryness under reduced pressure. The residue was dissolved in methylene chloride and washed with deionized water several times. The organic layer was separated, dried over anhydrous Na<sub>2</sub>SO<sub>4</sub>, filtered, and concentrated under vacuum. The residue was purified by flash chromatography on silica gel.

After numerous syntheses of this type, we found that it was not necessary to purify compounds **5** and **6** by column chromatography. In fact, these could be used directly in subsequent steps to provide satisfactory yields and purities of the target compounds **8**. Therefore, as long as adducts **4** and **7** were pure, one could avoid column chromatography on the other intermediates **5** and **6**.

**Anthracen-9-ylmethyl(2-hydroxyethyl)carbamic acid tert-butyl ester, 5a:** pale-yellow solid; mp 131–132 °C; yield 84%;  $R_f$  = 0.21 (acetone/hexane 1:4); <sup>1</sup>H NMR (CDCl<sub>3</sub>)  $\delta$  8.43 (s, 1H), 8.38 (br s, 2H), 8.01 (d, 2H), 7.43 (m, 4H), 5.50 (br s, 2H), 3.30 (t, 2H), 3.00 (br s, 3H, including –OH), 1.52 (br s, 9H). Anal. (C<sub>22</sub>H<sub>25</sub>NO<sub>3</sub>) C, H, N.

**Anthracen-9-ylmethyl(3-hydroxypropyl)carbamic acid tert-butyl ester, 5b:** unstable pale-yellow solid; yield 90%;  $R_f$  = 0.23 (acetone/hexane 1:4); <sup>1</sup>H NMR (CDCl<sub>3</sub>)  $\delta$  8.42 (s, 1H), 8.36 (d, 2H), 8.02 (d, 2H), 7.52 (m, 4H), 5.50 (br s, 2H), 3.25 (br s, 2H), 3.10 (br s, 2H), 1.62 (m, 11H). HRMS (FAB) calcd for C<sub>23</sub>H<sub>28</sub>NO<sub>3</sub> (M + H)<sup>+</sup>: 366.2069. Found: 366.2067.

**Anthracen-9-ylmethyl(4-hydroxybutyl)carbamic acid tert-butyl ester, 5c:** pale-yellow solid; mp 113–114 °C; yield 88%;  $R_f$  = 0.13 (acetone/hexane 12:88); <sup>1</sup>H NMR (CDCl<sub>3</sub>)  $\delta$  8.42 (s, 1H), 8.39 (d, 2H), 8.01 (d, 2H), 7.52 (m, 4H), 5.50 (br s, 2H), 3.25 (t, 2H), 2.80 (br s, 2H), 1.60 (br s, 9H), 1.20 (m, 4H). <sup>13</sup>C NMR  $\delta$  155.88, 131.52, 131.48, 129.45, 128.99, 126.53, 125.22, 124.32, 80.08, 62.35, 44.54, 41.28, 30.05, 28.94 (3C), 24.99. Anal. (C<sub>24</sub>H<sub>29</sub>NO<sub>3</sub>) C, H, N. HRMS (FAB) calcd for C<sub>24</sub>H<sub>29</sub>NO<sub>3</sub>Na (M + Na)<sup>+</sup>: 402.2045. Found: 402.2070.

**Anthracen-9-ylmethyl(5-hydroxypentyl)carbamic acid tert-butyl ester, 5d:** pale-yellow solid; mp 125–126 °C; yield 84%;  $R_f$  = 0.28 (acetone/hexane 1:4); <sup>1</sup>H NMR (CDCl<sub>3</sub>)  $\delta$  8.44 (s, 1H), 8.41 (d, 2H), 8.05 (d, 2H), 7.55 (m, 4H), 5.56 (br s, 2H), 3.38 (t, 2H), 2.82 (br s, 2H), 1.64 (br s, 9H), 1.25 (m, 4H), 0.98 (m, 2H); <sup>13</sup>C NMR  $\delta$  155.97, 131.56, 131.53, 129.43, 128.34, 126.51, 125.23, 124.43, 79.94, 62.85, 44.84, 41.41, 32.33, 28.96 (3C), 28.43, 23.14. Anal. (C<sub>25</sub>H<sub>31</sub>NO<sub>3</sub>) C, H, N. HRMS (FAB) calcd for C<sub>25</sub>H<sub>32</sub>NO<sub>3</sub> (M + H)<sup>+</sup>: 394.2382. Found: 394.2385.

**General Procedure for the Tosylation of 5 To Give 6.** A solution of the N-Boc protected (anthracen-9-ylmethyl)amino alcohol **5** (5 mmol) in 20 mL of dry pyridine was stirred at 0 °C for 10 min. *p*-Toluenesulfonyl chloride (TsCl, 7.5 mmol) was added in small portions over 30 min. The mixture was stirred for an additional hour, and the reaction flask was placed in a refrigerator (0–5 °C) overnight. The mixture was poured into 200 mL of ice/water, and a hemisolid (or viscous liquid) typically precipitated (or separated). After the upper layer was decanted off, the residue was dissolved in methylene chloride and washed several times with deionized water. The organic layer was separated, dried over anhydrous Na<sub>2</sub>SO<sub>4</sub>, filtered, and concentrated under vacuum. The residue was purified by flash chromatography on silica gel to give **6**.

**Toluene-4-sulfonic acid 3-(anthracen-9-ylmethyl-*tert*-butoxycarbonylamino)propyl ester, 6b:** unstable bright-yellow viscous liquid, yield 51%;  $R_f$  = 0.21 (acetone/hexane 1:4); <sup>1</sup>H NMR (CDCl<sub>3</sub>)  $\delta$  8.42 (s, 1H), 8.39 (d, 2H), 8.05 (d, 2H), 7.58 (m, 6H), 7.21 (d, 2H), 5.46 (s, 2H), 3.63 (t, 2H), 2.82 (t, 2H), 2.41 (s, 3H), 1.64 (br s, 11H). HRMS (FAB) calcd for C<sub>25</sub>H<sub>26</sub>NO<sub>3</sub>S (M + 2H – Boc)<sup>+</sup>: 420.1633. Found: 420.1642.

**Toluene-4-sulfonic acid 4-(anthracen-9-ylmethyl-*tert*-butoxycarbonylamino)butyl ester, 6c:** pale-yellow viscous liquid; yield 88%;  $R_f$  = 0.38, acetone/hexane 1:3; <sup>1</sup>H NMR

(CDCl<sub>3</sub>) δ 8.42 (s, 1H), 8.37 (d, 2H), 8.00 (d, 2H), 7.62 (d, 2H), 7.48 (m, 4H), 7.22 (d, 2H), 5.46 (s, 2H), 3.63 (t, 2H), 2.77 (br s, 2H), 2.40 (s, 3H), 1.48 (br s, 9H), 1.20 (br s, 4H). Anal. (C<sub>31</sub>H<sub>35</sub>NO<sub>5</sub>S·0.5H<sub>2</sub>O) C, H, N. HRMS calcd for C<sub>31</sub>H<sub>35</sub>NO<sub>5</sub>S M<sup>+</sup>: 533.2236. Found: 533.2236.

**Toluene-4-sulfonic acid 5-(anthracen-9-ylmethyl-tert-butoxycarbonylamino)pentyl ester, 6d:** pale-yellow viscous liquid; yield 88%; *R<sub>f</sub>* = 0.25, acetone/hexane 1:4; <sup>1</sup>H NMR (CDCl<sub>3</sub>) δ 8.42 (s, 1H), 8.36 (d, 2H), 8.00 (d, 2H), 7.63 (d, 2H), 7.46 (m, 4H), 7.22 (d, 2H), 5.47 (s, 2H), 3.73 (br s, 2H), 2.76 (br s, 2H), 2.40 (s, 3H), 1.48 (br s, 9H), 1.24 (br s, 2H), 1.20 (br s, 2H), 0.93 (br s, 2H). Anal. (C<sub>32</sub>H<sub>37</sub>NO<sub>5</sub>S·0.5H<sub>2</sub>O) C, H, N. HRMS (FAB) calcd for C<sub>32</sub>H<sub>38</sub>NO<sub>5</sub>S (M + H)<sup>+</sup>: 548.2471. Found: 548.2501.

**General Procedure for the Preparation of the N<sup>1</sup>-Boc Protected N<sup>1</sup>-(Anthracen-9-ylmethyl)triamines, 7.** The tosylated products **6** (1 mmol) and 1,4-diaminobutane or 1,3-diaminopropane (10 mmol) were dissolved in acetonitrile (10 mL), and then the mixture was stirred at 75 °C under N<sub>2</sub> overnight. After a check for the disappearance of the tosylate by TLC, the solution was concentrated under reduced pressure. The residue was dissolved in CH<sub>2</sub>Cl<sub>2</sub> (20 mL) and washed three times with saturated aqueous sodium carbonate. The organic layer was separated, dried over anhydrous sodium sulfate, filtered, and concentrated under vacuum. The residue was purified by flash chromatography on silica gel. The purified products **7** were used immediately for next step (BOC deprotection). The isolated yields ranged between 59% and 75%.

**General Procedure for the Preparation of the N<sup>1</sup>-(Anthracen-9-ylmethyl)triamines, 8.** The N<sup>1</sup>-Boc protected triamine **7** (0.5 mmol) was dissolved in ethanol (5 mL), and the mixture was stirred at 0 °C for 10 min. A 4 N aqueous HCl (8 mL) solution was added dropwise at 0 °C. The mixture was stirred at room temperature overnight. The solution was then concentrated under reduced pressure (while maintaining the water bath on the rotary evaporator below 60 °C), and a bright-yellow solid precipitated. The solids were washed several times with absolute ethanol and provided the pure target compounds **8b–g** as HCl salts. The <sup>1</sup>H NMR spectra of polyamine conjugates were measured in 0.5 mL of DMSO-*d*<sub>6</sub> and three drops of D<sub>2</sub>O. The use of DMSO-*d*<sub>6</sub>/D<sub>2</sub>O mixtures resulted in better spectral resolution (compared to using pure D<sub>2</sub>O as solvent). The <sup>13</sup>C NMR spectra of the triamines were measured in D<sub>2</sub>O to avoid the interference of DMSO carbon signals.

**N-(3-Aminopropyl)-N-anthracen-9-ylmethylpropane-1,3-diamine trihydrochloride salt, 8b:** bright-yellow solid, yield 98%; <sup>1</sup>H NMR (DMSO-*d*<sub>6</sub> + D<sub>2</sub>O) δ 8.80 (s, 1H), 8.40 (d, 2H), 8.22 (d, 2H), 7.75 (t, 2H), 7.62 (t, 2H), 5.23 (s, 2H), 3.40 (t, 2H), 3.05 (m, 4H), 2.96 (t, 2H), 2.18 (m, 2H), 2.00 (m, 2H); <sup>13</sup>C NMR δ 130.63, 130.45, 130.06, 129.47, 127.72, 125.50, 122.48, 120.06, 44.91, 44.82, 44.75, 43.08, 36.74, 23.98, 22.93. Anal. (C<sub>21</sub>H<sub>30</sub>Cl<sub>3</sub>N<sub>3</sub>) C, H, N. HRMS (FAB) calcd for C<sub>21</sub>H<sub>30</sub>Cl<sub>2</sub>N<sub>3</sub> (M + H - HCl)<sup>+</sup>: 394.1817. Found: 394.1806.

**N<sup>1</sup>-[3-(Anthracen-9-ylmethyl)amino]propyl]butane-1,4-diamine trihydrochloride salt, 8c:** bright-yellow solid, yield 98%; <sup>1</sup>H NMR (DMSO-*d*<sub>6</sub> + D<sub>2</sub>O) δ 8.80 (s, 1H), 8.42 (d, 2H), 8.20 (d, 2H), 7.72 (t, 2H), 7.62 (t, 2H), 5.23 (s, 2H), 3.42 (t, 2H), 3.05 (t, 2H), 2.98 (t, 2H), 2.82 (t, 2H), 2.20 (br s, 2H), 1.71 (br s, 4H); <sup>13</sup>C NMR (D<sub>2</sub>O) δ 130.57, 130.41, 130.01, 129.45, 127.71, 125.48, 122.46, 119.98, 47.27, 44.76, 44.66, 43.01, 39.03, 24.16, 23.00, 22.92. Anal. (C<sub>22</sub>H<sub>32</sub>Cl<sub>3</sub>N<sub>3</sub>·0.6H<sub>2</sub>O) C, H, N. HRMS (FAB) calcd for C<sub>22</sub>H<sub>32</sub>Cl<sub>2</sub>N<sub>3</sub> (M + H - HCl)<sup>+</sup>: 408.1973. Found: 408.1950.

**N-(3-Aminopropyl)-N-anthracen-9-ylmethylbutane-1,4-diamine trihydrochloride salt, 8d:** bright-yellow solid, yield 95%; <sup>1</sup>H NMR (DMSO-*d*<sub>6</sub> + D<sub>2</sub>O) δ 8.80 (s, 1H), 8.42 (d, 2H), 8.20 (d, 2H), 7.73 (t, 2H), 7.64 (t, 2H), 5.23 (s, 2H), 3.30 (t, 2H), 2.99 (m, 6H), 2.00 (m, 2H), 1.80 (m, 4H); <sup>13</sup>C NMR (D<sub>2</sub>O) δ 130.65, 130.37, 130.04, 129.48, 127.70, 125.51, 122.49, 120.30, 47.18 (2C), 44.78, 42.79, 36.81, 24.04, 23.14, 22.99. Anal. (C<sub>22</sub>H<sub>32</sub>Cl<sub>3</sub>N<sub>3</sub>) C, H, N. HRMS (FAB) calcd for C<sub>22</sub>H<sub>32</sub>Cl<sub>2</sub>N<sub>3</sub> (M + H - HCl)<sup>+</sup>: 408.1973. Found: 408.1958.

**N-(4-Aminobutyl)-N-anthracen-9-ylmethylbutane-1,4-diamine trihydrochloride salt, 8e:** bright-yellow solid, yield 91%; <sup>1</sup>H NMR (DMSO-*d*<sub>6</sub> + D<sub>2</sub>O) δ 8.80 (s, 1H), 8.42 (d, 2H), 8.20 (d, 2H), 7.70 (t, 2H), 7.61 (t, 2H), 5.23 (s, 2H), 3.30 (t, 2H), 2.93 (m, 4H), 2.82 (t, 2H), 1.78–1.60 (m, 8H); <sup>13</sup>C NMR (D<sub>2</sub>O) δ 130.62, 130.32, 130.01, 129.45, 127.67, 125.48, 122.48, 120.37, 47.17, 47.11, 47.00, 42.76, 39.03, 24.19, 23.14, 23.02 (2C). Anal. (C<sub>23</sub>H<sub>34</sub>Cl<sub>3</sub>N<sub>3</sub>·0.8H<sub>2</sub>O) C, H, N. HRMS (FAB) calcd for C<sub>23</sub>H<sub>32</sub>N<sub>3</sub> (M + H - 3HCl)<sup>+</sup>: 350.2590. Found: 350.2611.

**N-(3-Aminopropyl)-N-anthracen-9-ylmethylpentane-1,5-diamine trihydrochloride salt, 8f:** bright-yellow solid, yield 86%; <sup>1</sup>H NMR (DMSO-*d*<sub>6</sub> + D<sub>2</sub>O) δ 8.80 (s, 1H), 8.42 (d, 2H), 8.20 (d, 2H), 7.72 (t, 2H), 7.64 (t, 2H), 5.22 (s, 2H), 3.28 (t, 2H), 2.99 (m, 6H), 2.00 (m, 2H), 1.80 (m, 2H), 1.72 (m, 2H), 1.42 (m, 2H); <sup>13</sup>C NMR (D<sub>2</sub>O) δ 130.54, 130.23, 129.91, 129.39, 127.60, 125.42, 122.42, 120.30, 47.62, 47.54, 44.69, 42.56, 36.80, 25.28, 25.22, 24.01, 23.20. Anal. (C<sub>23</sub>H<sub>34</sub>Cl<sub>3</sub>N<sub>3</sub>·0.2H<sub>2</sub>O) C, H, N. HRMS (FAB) calcd for C<sub>23</sub>H<sub>34</sub>Cl<sub>2</sub>N<sub>3</sub> (M + H - HCl)<sup>+</sup>: 422.2130. Found: 422.2106.

**N-(4-Aminobutyl)-N-anthracen-9-ylmethylpentane-1,5-diamine trihydrochloride salt, 8g:** bright-yellow solid, yield 88%; <sup>1</sup>H NMR (DMSO-*d*<sub>6</sub> + D<sub>2</sub>O) δ 8.80 (s, 1H), 8.42 (d, 2H), 8.20 (d, 2H), 7.73 (t, 2H), 7.64 (t, 2H), 5.23 (s, 2H), 3.26 (t, 2H), 2.93 (br s, 4H), 2.82 (t, 2H), 2.00 (m, 2H), 1.80 (m, 2H), 1.72 (br s, 4H), 1.42 (m, 2H); <sup>13</sup>C NMR (D<sub>2</sub>O) δ 130.49, 130.21, 129.89, 129.38, 127.61, 125.41, 122.42, 120.23, 47.51, 47.46, 47.07, 42.50, 39.06, 25.29, 25.19, 24.22, 23.20, 23.04. Anal. (C<sub>24</sub>H<sub>36</sub>Cl<sub>3</sub>N<sub>3</sub>) C, H, N. HRMS (FAB) calcd for C<sub>24</sub>H<sub>36</sub>Cl<sub>2</sub>N<sub>3</sub> (M + H - HCl)<sup>+</sup>: 436.2286. Found: 436.2289.

**N-(Anthracen-9-ylmethyl)butylamine, Monohydrochloride, 11.** Compound **11** was synthesized in 58% yield by reductive amination of anthraldehyde and butylamine followed by treatment with 4 N aqueous HCl. These two procedures are described in the above general procedures for **4** and **8**, respectively.

**11:** yellow solid; yield 58%; *R<sub>f</sub>* = 0.5, methanol/chloroform, 1:20, + 1 drop of NH<sub>4</sub>OH; <sup>1</sup>H NMR (300 MHz, DMSO-*d*<sub>6</sub>) δ 9.1 (br s, 2H, NH<sub>2</sub> salt), 8.78 (s, 1H), 8.51 (d, 2H), 8.18 (d, 2H), 7.64 (m, 4H), 5.2 (br s, 2H), 3.2 (s, 2H), 1.73 (t, 2H), 1.36 (q, 2H), 0.92 (q, 3H); <sup>13</sup>C NMR (CDCl<sub>3</sub>) δ 131.6, 131.26, 130.55, 129.46, 128.05, 125.72, 123.89, 120.86, 46.05, 41.92, 28.48, 20.32, 13.79.

**Acknowledgment.** The authors thank the China Scholarship Council for partial support of C.W. This work was supported in part by the Elsa U. Pardee Foundation and the Florida Hospital Gala Endowed Program for Oncologic Research. The authors are also grateful to Ms. Fanta Konate for the synthesis of control **11**.

## References

- Phanstiel, O., IV; Price, H. L.; Wang, L.; Juusola, J.; Kline, M.; Shah, S. M. The Effect of Polyamine Homologation on the Transport and Cytotoxicity Properties of Polyamine-(DNA-Intercalator) Conjugates. *J. Org. Chem.* **2000**, *65*, 5590–5599.
- Wang, L.; Price, H. L.; Juusola, J.; Kline, M.; Phanstiel, O., IV. The Influence of Polyamine Architecture on the Transport and Topoisomerase II Inhibitory Properties of Polyamine DNA-Intercalator Conjugates. *J. Med. Chem.* **2001**, *44*, 3682–3691.
- Sugiyama, S.; Matsuo, Y.; Maenaka, K.; Vassilyev, D. G.; Matsushima, M.; Kashiwagi, K.; Igarashi, K.; Morikawa, K. The 1.8-Å X-ray structure of the *Escherichia coli* PotD protein complexed with spermidine and the mechanism of polyamine binding. *Protein Sci.* **1996**, *5*, 1984–1990.
- Vassilyev, D. G.; Tomitori, H.; Kashiwagi, K.; Morikawa, K.; Igarashi, K. Crystal structure and mutational analysis of the *Escherichia coli* putrescine receptor. Structural basis for substrate specificity. *J. Biol. Chem.* **1998**, *273*, 17604–17609.
- Bergeron, R. J.; Feng, Y.; Weimar, W. R.; McManis, J. S.; Dimova, H.; Porter, Carl; Raisler, B.; Phanstiel, O. A Comparison of Structure-Activity Relationships between Spermidine and Spermine Analogue Antineoplastics. *J. Med. Chem.* **1997**, *40*, 1475–1494.
- Cullis, P. M.; Green, R. E.; Merson-Davies, L.; Travis, N. Probing the mechanism of transport and compartmentalisation of polyamines in mammalian cells. *Chem. Biol.* **1999**, *6*, 717–729 and references therein.



- (7) Kramer, D. L.; Miller, J. T.; Bergeron, R. J.; Khomutov, R.; Khomutov, A.; Porter, C. W. Regulation of polyamine transport by polyamines and polyamine analogs. *J. Cell. Physiol.* **1993**, *155*, 399–407.
- (8) Kashiwagi, K.; Endo, H.; Kobayashi, H.; Takio, K.; Igarashi, K. Spermidine-preferential uptake system in *Escherichia coli*. ATP hydrolysis by PotA protein and its association with membrane. *J. Biol. Chem.* **1995**, *270*, 25377–25382.
- (9) Kashiwagi, K.; Miyamoto, S.; Nukui, E.; Kobayashi, H.; Igarashi, K. Functions of potA and potD proteins in spermidine-preferential uptake system in *Escherichia coli*. *J. Biol. Chem.* **1993**, *268*, 19358–19363.
- (10) Tomitori, H.; Kashiwagi, K.; Sakata, K.; Kakinuma, Y.; Igarashi, K. Identification of a gene for a polyamine transport protein in yeast. *J. Biol. Chem.* **1999**, *274*, 3265–3267.
- (11) (a) Bergeron, R. J.; Wiegand, J.; McManis, J. S.; Weimar, W. R.; Smith, R. E.; Algee, S. E.; Fannin, T. L.; Slusher, M. A.; Snyder, P. S. Polyamine Analogue Antidiarrheals: A Structure–Activity Study. *J. Med. Chem.* **2001**, *44*, 232–244. (b) Bergeron, R. J.; Yao, G. W.; Yao, H.; Weimar, W. R.; Sninsky, C. A.; Raisler, B.; Feng, Y.; Wu, Q.; Gao, F. Metabolically Programmed Polyamine Analogue Antidiarrheals. *J. Med. Chem.* **1996**, *39*, 2461–2471. (c) Bergeron, R. J.; Neims, A. H.; McManis, J. S.; Hawthorne, T. R.; Vinson, J. R. T.; Bortell, R.; Ingeno, M. J. Synthetic polyamine analogs as antineoplastics. *J. Med. Chem.* **1988**, *31*, 1183–1190. (d) Casero, R. A., Jr.; Woster, P. M. Terminally Alkylated Polyamine Analogues as Chemotherapeutic Agents. *J. Med. Chem.* **2001**, *44*, 1–26 and references therein.
- (12) Delcros, J.-G.; Tomasi, S.; Carrington, S.; Martin, B.; Renault, J.; Blagbrough, I. S.; Uriac, P. Effect of spermine conjugation on the cytotoxicity and cellular transport of acridine. *J. Med. Chem.* **2002**, *45*, 5098–5111.
- (13) Azzam, T.; Eliyahu, H.; Shapira, L.; Linial, M.; Barenholz, Y.; Domb, A. J. Polysaccharide–Oligoamine Based Conjugates for Gene Delivery. *J. Med. Chem.* **2002**, *45*, 1817–1824.
- (14) Stark, P. A.; Thrall, B. D.; Meadows, G. G.; Abdul-Monem, M. M. Synthesis and evaluation of novel spermidine derivatives as targeted cancer chemotherapeutic agents. *J. Med. Chem.* **1992**, *35*, 4264–4269.
- (15) Cohen, G. M.; Cullis, P.; Hartley, J. A.; Mather, A. Symons, M. C. R.; Wheelhouse, R. T. Targeting of Cytotoxic Agents by Polyamines: Synthesis of a Chloroambucil–Spermidine Conjugate. *J. Chem. Soc., Chem. Commun.* **1992**, 298–300.
- (16) Cai, J.; Soloway, A. H. Synthesis of Carboranyl Polyamines for DNA Targeting. *Tetrahedron Lett.* **1996**, *37*, 9283–9286.
- (17) Ghaneilhosseini, H.; Tjarks, W.; Sjöberg, S. Synthesis of Novel Boronated Acridines and Spermidines as Possible Agents for BNCT. *Tetrahedron* **1998**, *54*, 3877–3884.
- (18) Blagbrough, I. S.; Geall, A. J. Homologation of Polyamines in the Synthesis of Lipo-Spermine Conjugates and Related Lipoplexes. *Tetrahedron Lett.* **1998**, 443–446.
- (19) Blagbrough, I. S.; Geall, A. J. Practical Synthesis of Unsymmetrical Polyamine Amides. *Tetrahedron Lett.* **1998**, 439–442.
- (20) Cullis, P. M.; Merson-Davies, L.; Weaver, R. Mechanism and reactivity of chlorambucil and chlorambucil–spermidine conjugate. *J. Am. Chem. Soc.* **1995**, *117*, 8033–8034.
- (21) Aziz, S. M.; Yatin, M.; Worthen, D. R.; Lipke, D. W.; Crooks, P. A. A novel technique for visualising the intracellular localization and distribution of transported polyamines in cultured pulmonary artery smooth muscle cells. *J. Pharm. Biomed. Anal.* **1998**, *17*, 307–320.
- (22) Saab, N. H.; West, E. E.; Bieszk, N. C.; Preuss, C. V.; Mank, A. R.; Casero, R. A.; Woster, P. M. Synthesis and Evaluation of Polyamine Analogues as Inhibitors of Spermidine/Spermine–N<sup>1</sup>-Acetyltransferase (SSAT) and as Potential Antitumor Agents. *J. Med. Chem.* **1993**, *36*, 2998–3004.
- (23) (a) Chaney, S. E.; Kobayashi, K.; Goto, R.; Digenis, G. A. Tumor selective enhancement of radioactivity uptake in mice treated with  $\alpha$ -difluoromethylornithine prior to administration of <sup>14</sup>C-putrescine. *Life Sci.* **1983**, *32*, 1237–1241. (b) Heston, W. D. W.; Kadmon, D.; Covey, D. F.; Fair, W. R. Differential effect of  $\alpha$ -difluoromethylornithine on the in vivo uptake of <sup>14</sup>C-labeled polyamines and methylglyoxal bis(guanyldiazide) by a rat prostate-derived tumor. *Cancer Res.* **1984**, *44*, 1034–1040. (c) Redgate, E. S.; Grudziak, A. G.; Deutsch, M.; Boggs, S. S. Difluoromethylornithine enhanced uptake of tritiated putrescine in 9L rat brain tumors. *Int. J. Radiat. Oncol., Biol., Phys.* **1997**, *38*, 169–174.
- (24) (a) Kumar, C. V.; Asuncion, E. H. DNA Binding Studies and Site Selective Fluorescence Sensitization of an Anthryl Probe. *J. Am. Chem. Soc.* **1993**, *115*, 8547–8553. (b) Rodger, A.; Taylor, S.; Adlam, G.; Blagbrough, I. S.; Haworth, I. S. Multiple DNA Binding Modes of Anthracene-9-Carbonyl–N<sup>1</sup>-Spermine. *Bioorg. Med. Chem.* **1995**, *3*, 861–872.
- (25) Wang, C.; Abboud, K. A.; Phanstiel, O. IV Synthesis and Characterization of N1-(4-toluenesulfonyl)-N1-(9-anthracenemethyl)triamines. *J. Org. Chem.* **2002**, *67*, 7865–7868.
- (26) Porter, C. W.; Cavanaugh, P. F.; Ganis, B.; Kelly, E.; Bergeron, R. J. Biological properties of N-4 and N-1, N-8-spermidine derivatives in cultured L1210 leukemia cells. *Cancer Res.* **1985**, *45*, 2050–2057.
- (27) Mandel, J. L.; Flintoff, W. F. Isolation of mutant mammalian cells altered in polyamine transport. *J. Cell. Physiol.* **1978**, *97*, 335–344.
- (28) Byers, T. L.; Wechter, R.; Nuttall, M. E.; Pegg, A. E. Expression of a human gene for polyamine transport in Chinese hamster ovary cells. *Biochem. J.* **1989**, *263*, 745–752.
- (29) Porter, C. W.; Ganis, B.; Vinson, T.; Marton, L. J.; Kramer, D. L.; Bergeron, R. J. Comparison and characterization of growth inhibition in L1210 cells by  $\alpha$ -difluoromethylornithine, an inhibitor of ornithine decarboxylase, and N1,N8-bis(ethyl)spermidine, an apparent regulator of the enzyme. *Cancer Res.* **1986**, *46*, 6279–6285.
- (30) Bergeron, R. J.; McManis, J. S.; Weimar, W. R.; Schreier, K. M.; Gao, F.; Wu, Q.; Ortiz-Ocasio, J.; Luchetta, G. R.; Porter, C.; Vinson, J. R. T. The role of charge in polyamine analog recognition. *J. Med. Chem.* **1995**, *38*, 2278–2285.
- (31) Porter, C.; Miller, J.; Bergeron, R. J. Aliphatic chain-length specificity of the polyamine transport system in ascites L1210 leukemia cells. *Cancer Res.* **1984**, *44*, 126–128.
- (32) Xia, C. Q.; Yang, J. J.; Ren, S.; Lien, E. J. QSAR analysis of polyamine transport inhibitors in L1210 cells. *J. Drug Targeting* **1998**, *6*, 65–77.
- (33) O'Sullivan, M. C.; Golding, B. T.; Smith, L. L.; Wyatt, I. Molecular features necessary for the uptake of diamines and related compounds by the polyamine receptor of rat lung slices. *Biochem. Pharmacol.* **1991**, *41*, 1839–1848.
- (34) Bergeron, R. J.; McManis, J. S.; Liu, C. Z.; Feng, Y.; Weimar, W. R.; Luchetta, G. R.; Wu, Q.; Ortiz-Ocasio, J.; Vinson, J. R. T.; Kramer, D.; Porter, C. Antiproliferative Properties of Polyamine Analogues: A Structure–Activity Study. *J. Med. Chem.* **1994**, *37*, 3464–3476.
- (35) Soulet, D.; Covassin, L.; Kaouass, M.; Charest-Gaudreault, R.; Audette, M.; Poulin, R. Role of endocytosis in the internalisation of spermidine–C2-BODIPY, a highly fluorescent probe of polyamine transport. *Biochem. J.* **2002**, *367*, 347–357.
- (36) Kuksa, V.; Buchan, R.; Lin, P. K. T. Synthesis of Polyamines, Their Derivatives, Analogues and Conjugates. *Synthesis* **2000**, No. 9, 1189–1207.
- (37) Mosmann, T. Rapid colorimetric assay for cellular growth and survival: application to proliferation and cytotoxicity assays. *J. Immunol. Methods* **1983**, *65*, 55–63.
- (38) Clément, S.; Delcros, J. G.; Feuerstein, B. G. Spermine uptake is necessary to induce haemoglobin synthesis in murine erythroleukemia cells. *Biochem. J.* **1995**, *312*, 933–938.
- (39) Cheng, Y.-C.; Prusoff, W. H. Relationship between the inhibition constant (K<sub>i</sub>) and the concentration of inhibitor which causes 50% inhibition (IC<sub>50</sub>) of an enzymatic reaction. *Biochem. Pharmacol.* **1973**, *22*, 3099–3108.
- (40) Torossian, K.; Audette, M.; Poulin, R. Substrate protection against inactivation of the mammalian polyamine transport system by 1-ethyl-3-(3-dimethylaminopropyl)-carbodiimide. *Biochem. J.* **1996**, *319*, 21–26.
- (41) Covassin, L.; Desjardins, M.; Charest-Gaudreault, R.; Audette, M.; Bonneau, M. J.; Poulin, R. Synthesis of spermidine and norspermidine dimers as high affinity polyamine transport inhibitors. *Bioorg. Med. Chem. Lett.* **1999**, *9*, 1709–1714.
- (42) Bergeron, R. J.; Müller, R.; Bussenius, J.; McManis, J. S.; Merriman, R. L.; Smith, R. E.; Yao, H.; Weimar, W. R. Synthesis and Evaluation of Hydroxylated Polyamine Analogues as Antiproliferatives. *J. Med. Chem.* **2000**, *43*, 224–235.

JM030028W